

# TECHNICAL CHALLENGES OF THE LCLS-II CW X-RAY FEL\*

T.O. Raubenheimer<sup>#</sup> for the LCLS-II Collaboration, SLAC, Menlo Park, CA 94025, USA

## Abstract

The LCLS-II will be a CW X-ray FEL upgrade to the existing LCLS X-ray FEL at the SLAC National Accelerator Laboratory (SLAC). This paper will describe the overall layout and describe the technical challenges that the upgrade project faces.

## INTRODUCTION

The LCLS-II is an X-ray Free-Electron Laser (FEL) which will upgrade the LCLS FEL at SLAC. The LCLS-II is designed to deliver photons between 200 eV and 5 keV at repetition rates as high as 1 MHz (929 kHz) using a superconducting RF linac (SCRf) linac while still providing pulses at short wavelengths and high X-ray pulse energy over the photon range of 1 to 25 keV using the existing 120 Hz copper RF (CuRF) LCLS linac.

The LCLS-II project is being constructed by a collaboration of US laboratories consisting of Argonne National Lab. (ANL), Cornell University (CU), Fermilab (FNAL), Jefferson Lab. (JLab), Lawrence Berkeley National Lab. (LBNL), and SLAC. In addition, the project has substantial assistance from the EuXFEL project as well as the other international laboratories focused on SCRf development and XFEL's.

will be transported to the existing LCLS Undulator Hall where, to cover the full photon-energy range, the existing LCLS fixed gap undulator will be removed and the facility will install two variable-strength (gap-tunable) undulators, one dedicated to the production of Soft X-rays (SXR Undulator) from 0.2 – 1.3 keV and one dedicated to production of Hard X-rays (HXR Undulator) from 1.0 – 25.0 keV. The facility will also allow the possibility of generating near transform-limited pulses using self-seeding as well as downstream monochromators.

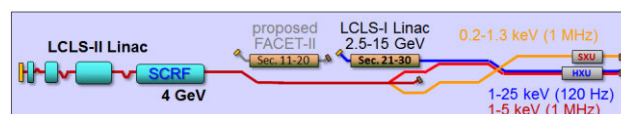


Figure 2: Schematic layout of the LCLS-II project.

As illustrated in Figure 2, the facility is constructed to either deliver high-rate beam from the SCRf linac to both the SXR and HXR undulators, or to deliver the high-rate beam to the SXR undulator and deliver beam from the existing copper CuRF linac at 120 Hz to the HXR undulator.

The LCLS-II will have the high peak brightness capability and flexibility of LCLS while also having the ability to provide MHz rate beams from a CW SCRf linac. The operating regimes are:

1. Soft X-ray photons from SASE and self-seeding between 0.2 and 1.3 keV at MHz rates, with an average X-ray power in excess of 20 Watts;
2. Hard X-ray photons from SASE between 1.0 and 5.0 keV at MHz rates with an average X-ray power in excess of 20 Watts and with the possibility of a future upgrade to self-seeding operation at energies between 1 and 4 keV;
3. Hard X-ray photons with SASE between 1 and 25 keV and self-seeding between 4 keV and 13 keV at 120 Hz, with mJ-class pulses and performance comparable to or exceeding that of LCLS.

Bunches from the SCRf linac will be directed to either the HXR or SXR with a high rate magnetic kicker that will allow independent control of the beam rate being delivered to either undulator. The SCRf linac will be intrinsically more stable than the LCLS linac and the energy stability of the electron beams is specified to be <0.01% rms which >10x more stable than that from the CuRF linac. The timing stability in the initial implementation of LCLS-II is specified to be better than 20 fs rms and is expected to be less than 10 fs rms. It is expected that the stability of the SCRf beams will be

Content from this work may be used under the terms of the CC BY 3.0 license (© 2015). Any distribution of this work must maintain attribution to the author(s), title of the work, publisher, and DOI.



Figure 1: Schematic of the LCLS facility with the LCLS-II SCRf upgrade shown in blue.

The SCRf linac will be installed in the first third (1 km) of the SLAC linac tunnel and a bypass line will bring the high rate beam around the middle third of the existing linac and the existing LCLS CuRF linac as illustrated in Figure 1. Beams from both the CuRF and the SCRf linac

\* Work supported by DOE Contract: DE-AC02-76-SF00515  
<sup>#</sup> torr@stanford.edu

improved after the initial operation with the implementation of additional feedback systems that are possible due to the very high repetition rates of the linac.

The LCLS-II will be flexible in its operating modes consistent with the maximum x-ray beam power, the maximum electron beam power to the BSY and undulator dumps, the maximum repetition rate and the range of bunch charges. As noted above, the HXR can be fed from either the SCRF linac or the CuRF linac, while the SXR can be fed only from the SCRF linac. The BSY Beam Spreader can direct the SCRF linac beam arbitrarily toward either undulator or to the BSY dump. The design does not presently include the capability of delivering different bunch charges or peak currents to the two undulators simultaneously, however that capability may be developed in the future.

The beams from the CuRF linac at 120 Hz will retain all of the flexible operating modes that are being developed at LCLS. These include pulse-length control, two-color pulses and two pulses with delay at the 100 fs scale. New techniques are being developed as well which may allow pulse-by-pulse pulse length control and limited shaping of the x-ray pulses. Many of these techniques will be implemented on the SCRF linac as well however these capabilities are beyond the baseline project and will take time after initial operation to develop the full capability.

### TECHNICAL CHALLENGES

The LCLS-II will be similar to the design of the LCLS. The primary differences are also related to the technical challenges the project faces:

1. The CW SCRF linac
2. High brightness CW injector
3. Variable gap undulators
4. High power beams
5. Beam dynamics of high brightness low energy beams

These issues will be described further below.

#### SCRF Linac

The LCLS-II SCRF linac will be constructed from 35 1.3 GHz cryomodules (CM), each containing eight 9-cell cavities. Like the LCLS linac, the linac will contain a Laser Heater at 100 MeV to suppress the micro-bunching stability and two bunch compressors, BC1 at 250 MeV and BC2 at 1.6 GeV as illustrated in Figure . . In addition, two 3.9 GHz CM with eight 9-cell cavities will be installed upstream of BC1 to linearize the longitudinal phase space. The total installed 1.3 GHz voltage will be 4.5 GV but with a margin of 6% for failed cavities and the rf phases for bunch compression, the maximum beam energy is 4.15 GeV. Parameters are listed in Table 1.

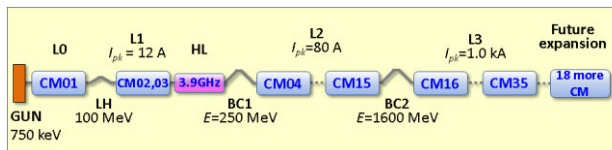


Figure 3: Schematic of LCLS-II SCRF linac.

Table 1: SCRF 1.3 GHz Linac Parameters

<b>Gradient</b>	16 MV/m
<b>Average Q<sub>0</sub></b>	2.7x10 <sup>10</sup>
<b>Num. Cavities</b>	280 (35 CM)
<b>Total voltage</b>	4.48 GV
<b>Max. Beam Energy</b>	4.15 GeV
<b>Max. bunch rep. rate</b>	929 kHz
<b>Max. bunch charge</b>	300 pC

The SCRF cavities are based on the TESLA design pioneered at DESY and the CM's are similar to those developed for the ILC and EuXFEL program but modified for CW operation.

In a CW SCRF linac, the heat load is dominated by the rf losses in the cavities which scales as Grad<sup>2</sup>/Q. The state-of-art at 1.3 GHz is the EuXFEL cavities which achieve Q's of roughly 1.5x10<sup>10</sup> and gradient's in excess of 25 MV/m. The dynamic heat load due to these cavities is fine at the low duty-cycle of the EuXFEL but would be prohibitive in the CW LCLS-II. To minimize the rf losses, the LCLS-II project is supporting R&D aimed at developing Q's in excess of 2.7x10<sup>10</sup> at a gradient of 16 MV/m.

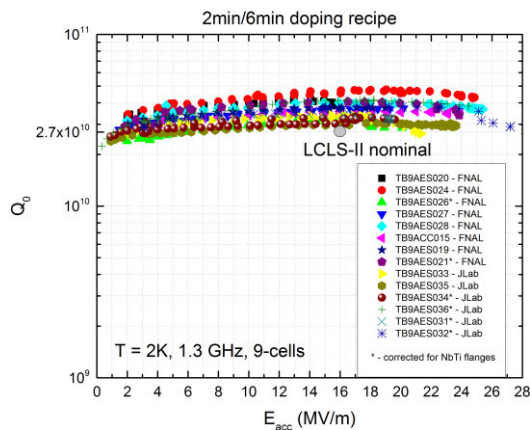


Figure 4: Q versus gradient for N-doped 9-cell cavities tested at FNAL and JLab.

This enormous challenge is being met using the Nitrogen-doping technique that has been developed at FNAL. This technique has improved the Q's of the 1.3 GHz 9-cell cavities by more than a factor of two as illustrated in Figure 4. While the cavity processing has

Content from this work may be used under the terms of the CC BY 3.0 licence (© 2015). Any distribution of this work must maintain attribution to the author(s), title of the work, publisher, and DOI.

proceeded very well, there are still challenges in translating these benefits to a full CM and the LCLS-II will likely design for additional cryogenic overhead to ensure success in meeting the design goal of a 4 GeV electron beam. An excellent summary of the present high-Q SCRF cavity status can be found in Ref. [1].

The cavity processing procedure is being developed at FNAL, JLab, and CU. FNAL and JLab will each build one prototype 8-cavity CM by the end of 2015 and these will be verified during the first half of 2016. The construction of the rest of the CM's for the LCLS-II will be shared between FNAL and JLab.

The SCRF linac will be cooled with one or two 4 kW cryoplants, depending on how successfully the high-Q results are transferred to the CM's. The cryoplant(s) will be similar to that built for the JLab 12 GeV upgrade [2] and will provide cooling for 4 kW at 2°K. The plant is being designed by JLab while FNAL is designing the cryo-distribution systems. The plants will be located roughly halfway along the linac (adjacent to BC2) and will feed cryogenics both upstream toward the injector and downstream. The layout for a single plant is illustrated in Figure 5.

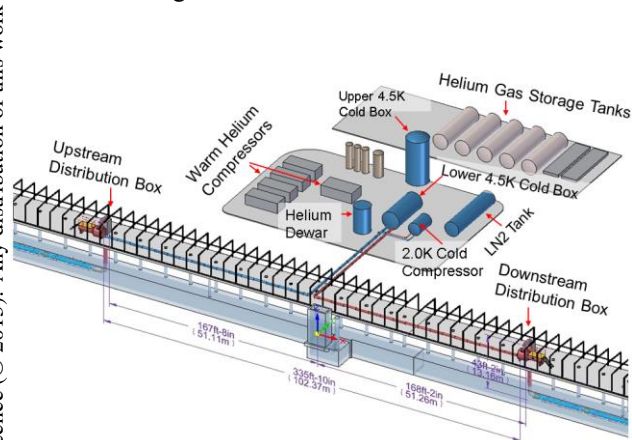


Figure 5: Schematic of a single cryoplant for the LCLS-II SCRF linac.

The SCRF linac is being designed to accelerate 300  $\mu$ A up to >4GeV for 1.2 MW of beam power, which is sufficient to ultimately generate more than 100 Watts of X-rays in up to 10 individual undulator beamlines. The initial LCLS-II configuration will be limited to a maximum power of 250 kW, supplying beam to only the first two undulators. It only includes sufficient RF power to accelerate 100 uA up to 4 GeV at 16 MV/m.

The two configurations considered for the RF power configuration were a single high-power source powering multiple (48) cavities or a single-source, single cavity configuration. While the single-source, multiple-cavity configuration was expected to be a significant cost savings, the project will be based on the single-source, single cavity configuration because it is expected to have significantly better control of the cavity fields. The RF power will be supplied by 3.8 kW solid-state amplifiers and the LLRF system for the LCLS-II is described in Ref. [3].

## High Brightness CW Injector

The performance of an FEL depends critically on the incoming electron beam brightness. For CW operation, a normal conducting high gradient rf gun is not possible and, while lots of potential exists, superconducting rf guns have not yet demonstrated the desired brightness.

Instead, the LCLS-II will use a low voltage rf gun very similar to the 186 MHz rf gun being developed as part of the APEX project at LBNL [4]. The normal-conducting photo-cathode gun will provide a beam of 750 keV which is then bunched with a 1.3 GHz normal conducting buncher cavity before being injected into a standard 1.3 GHz CM where it is captured and accelerated to 100 MeV. It is expected that the relatively high voltage of the rf gun will provide a higher beam brightness than a DC gun operating at 400 to 500 kV.

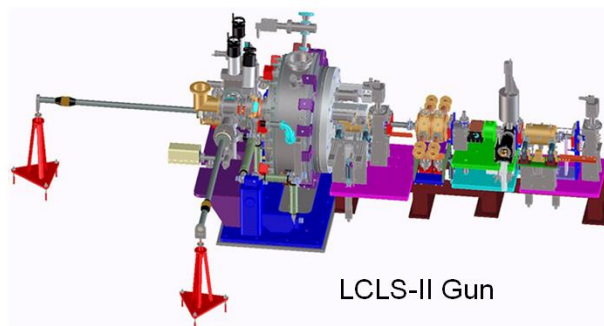


Figure 6: Schematic of the LCLS-II injector, based on the LBNL APEX rf gun.

The APEX project has demonstrated the operation of the rf gun at 800 kV and is in the process of installing the 1.3 GHz buncher cavity and downstream accelerator structures to accelerate the beam to 30 MeV and verify the beam brightness. Brightness measurements are expected in the Fall of 2015.

In parallel, the Cornell DC gun which was developed for an Energy Recovery Linac [5], has been operated at 400 kV and the beam brightness has been measured for bunch charges across the LCLS-II operating range of 10 – 300 pC using a new NaKSb cathode [6]. The gun was optimized to meet the LCLS-II emittance and peak current requirements and the studies provided an excellent benchmark of the ASTRA and GPT gun simulation codes, providing confidence in the LCLS-II injector design.

The baseline cathode will be Cs<sub>2</sub>Te illuminated in the UV. The laser system has been sized for a 0.5% QE and the emittance performance is based on a 1 mm-mrad per mm thermal emittance. Measurements at the APEX rf gun of the thermal emittance and QE exceed the design specifications.

In addition, alkali-antimonide cathodes are being developed around the world and, if proven robust, will be adopted by the LCLS-II project to improve the beam emittance and simplify the gun laser system. As noted, measurements on the Cornell dc gun were made using a

NaKSb cathode with a thermal emittance  $\sim 30\%$  smaller than the typical  $\text{Cs}_2\text{Te}$  cathodes of 0.8 mm-mrad/mm.

### Variable Gap Undulators

As noted, the SXR undulator can be fed from the SCRF linac, while the HXR undulator can be fed from either the SCRF or the CuRF linacs, although not from both simultaneously. The undulators will be installed side-by-side in the existing LCLS Undulator Hall. A schematic of the undulator layout appears in Figure 7.

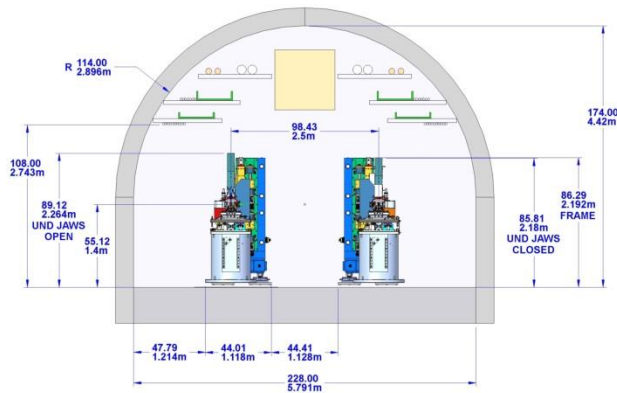


Figure 7: Schematic of HXR and SXR undulators in the LCLS Undulator Hall.

Both undulators are variable-gap hybrid permanent-magnet undulators. The HXR undulator has a period of 26 mm, close to that of the existing LCLS undulator, while the SXR undulator has a period of 39 mm. The maximum length of the existing LCLS Undulator Hall is roughly 150 meters. This will allow for the installation of up to 35 segments for the HXR, with each segment being 3.4 meters long followed by an interspace of 1.0 meters for a quadrupole, phase shifter, RF BPM, and  $x$  and  $y$  steering coils. To support self-seeding, two of these undulator slots will be reserved for self-seeding monochromators. The baseline will include 32 HXR segments plus two self-seeding slots, one of which contains the existing LCLS HXR self-seeding monochromator [7]; the other is reserved for a future upgrade.

The SXR undulator can be shorter, and there will be 21 SXR undulator segments plus one empty slot for the self-seeding monochromator which will be based on the LCLS SXRSS monochromator but modified for higher average power with a resolving power  $>10,000$ . Development of the SXRSS monochromator is ongoing. The last three SXR undulator slots are reserved for the future installation of polarization control undulators such as DELTA undulators [8], and the space upstream of the SXR undulator may be used for future seeding installations or additional undulators for two-color X-ray generation or other upgrades.

The baseline LCLS-II undulators are being developed at LBNL [9]. The undulator parameters are listed in Table 2. A 3.4-meter prototype has been constructed and is shown in Figure 8.

Table 2: Parameters for the HXR and SXR Undulators

	HXR	SXR
<b>Period</b>	26 mm	39 mm
<b>Mag. Material</b>	$\text{Nd}_2\text{Fe}_{14}\text{B}$	$\text{Nd}_2\text{Fe}_{14}\text{B}$
<b>Max. K</b>	2.44	5.48
<b>Min. gap</b>	7.2 mm	7.2 mm
<b>Seg. Length</b>	3.4 m	3.4 m
<b>Num. Segments</b>	32	21
<b>Interspace Len.</b>	1 m	1 m
<b>Total Length</b>	96 m	140 m

The LCLS-II project is also exploring the option of a horizontal-gap, vertically polarizing undulator (VPU) which would significantly reduce losses in the horizontally deflecting optics downstream of the HXR undulator at photon energies between 5 and 10 keV. A prototype VPU is being developed at Argonne National Laboratory with testing expected in the Fall of 2015 [9].

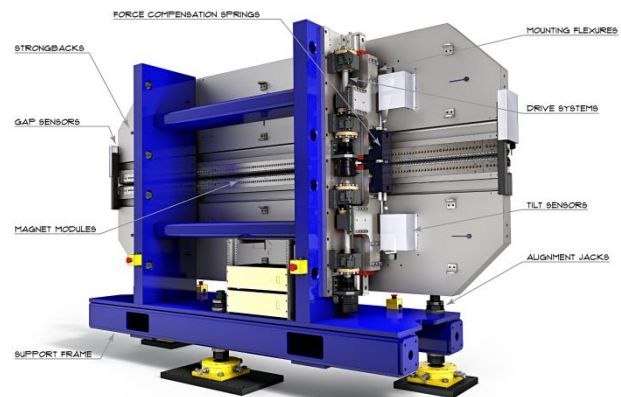


Figure 8: Prototype LCLS-II variable gap undulator.

### High Beam Power

The LCLS-II SCRF linac is being designed to deliver 1.2 MW at 4 GeV of electron beam power although the initial rf system will only support a maximum of 400 kW at 4 GeV. Each of the two undulator systems (SXR and HXR) is design to operate with up to 120 kW of electron beam power which can generate as much as 1 kW of X-rays. The X-ray transport systems are designed for a maximum of 200 W across the operating spectrum. Furthermore, to ensure a 10-year operating lifetime, beam loss in the hybrid permanent magnet undulator systems must be limited to an average of 12 mW, i.e.  $1 \times 10^{-7}$  of the maximum beam power. Control of the electron and X-ray beam power requires careful design of passive and active systems.

SLAC has operating experience with high power beams and the beam dumps and operating systems are being designed with this experience. The beam dumps are water-cooled dumps based on previous designs and the

collimation system to limit the beam losses in the undulators is a four-stage design in which each stage will collimate in ( $x$ ,  $x'$ ,  $y$ ,  $y'$  and  $\Delta E$ ). Additional collimation of parasitical (off-time) buckets may also be implemented.

Because of transients induced when changing the beam current profile and timing in the SCRF linac, the time required to change the rate is limited by the damping time of the feedback systems. When operating with a high-repetition-rate beam in the linac, we expect that this time will be a fraction of a second. The time needed to switch between the SCRF linac and the CuRF linac will be dominated by the time required to change out the DC magnets and re-establish the electron beam. This should take less than one hour. To simplify operations, the beam power in the undulators is controlled using a magnetic kicker located at the end of the SCRF linac. This will allow the full power linac beam to be tuned up onto a high power dump before beam is taken to and through the undulators. Using the kicker, the rate to each of the undulators can be rapidly controlled from single-shot to maximum rate.

The very high average power of the accelerated CW electron beam can damage components within a few 100  $\mu\text{s}$ . For this reason, several accelerator operating modes are envisioned for initial low-power commissioning, recovery from RF trips, recovery from beam-loss trips, and startup from shut-down periods. The Machine Protection System (MPS) is being designed with a 100  $\mu\text{s}$  trip rate which is facilitated using the segmented design; if a fault arises near the undulator systems, beam can first be put onto the high power linac beam dump and then stopped at the electron source.

### Beam Dynamics

The LCLS-II beam from the CuRF linac is very similar to that of the operating LCLS and thus is well quantified however understanding the beam from the SCRF linac has a new set of challenges. As noted, the design of the linac is similar to that of the LCLS with a laser heater and two-stage bunch compressor.

To ensure the performance of the LCLS-II, analytic studies and detailed Start-to-End (S2E) simulations are being performed using the IMPACT [10] and Elegant [11] tracking codes and the Genesis v1.3 FEL simulation code [12]. The low energy of the beam from the SCRF linac and the long transport makes the space charge and micro-bunching effects more significant than in LCLS. A number of new effects driven by space charge have been simulated including micro-bunching effects driven by transverse space charge in dispersive regions and the impact of longitudinal nonlinearities [13].

These new effects have led to design modifications to moderate their impact. With these changes, it is believed that the high-rate HXR and SXR FEL's will exceed specification of  $>20$  W across the parameter range as illustrated in Figure 9.

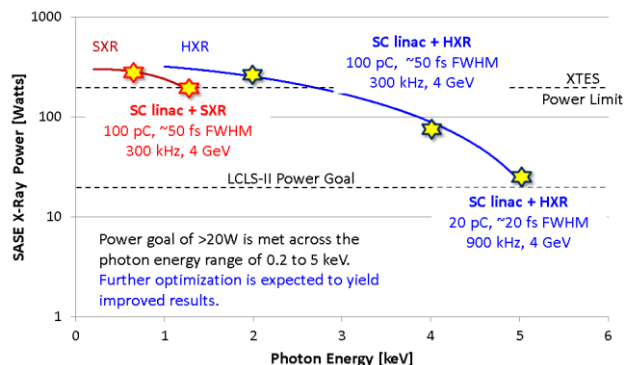


Figure 9: SASE X-ray average power from LCLS-II high-rate beam.

In parallel, experimental studies are being performed on the LCLS to verify the simulation codes in a parameter regime similar to that expected for the LCLS-II operation [14]. When complete, this confirmation is expected to provide significant confidence in the LCLS-II accelerator design.

## CONCLUSION

The LCLS-II project is developing an upgrade to the LCLS X-ray FEL at SLAC that is based on a 4 GeV SCRF linac and two variable-gap undulators. The project is being constructed by a collaboration of six institutions from across the US. The design of the accelerator and required hardware is well advanced and proceeding toward first X-rays at the end of 2019.

## REFERENCES

- [1] A. Grassellino, Proc. of IPAC'15, MOYGB2 (2015) and references within.
- [2] A. Freyberger, Proc. of IPAC'15, MOXGB2 (2015) and references within.
- [3] C. Hovater, Proc. of IPAC'15, MOPWI021 (2015).
- [4] F. Sannibale et al., PRST-AB **15**, 103501 (2012).
- [5] C. Gulliford et al., PRST-AB **16**, 073401 (2013).
- [6] C. Gulliford, et al, <http://arxiv.org/abs/1501.04081> (2015).
- [7] J. Amann, et al., Nature Photonics **6**, 693 (2012).
- [8] A. Temnykh, Phys. Rev. ST Accel. Beams **11**, 120702 (2008).
- [9] E. Gluskin, Proc. of IPAC'15, TUXC1 (2015) and references within.
- [10] J. Qiang, et al., PRST-AB **12**, 100702 (2009).
- [11] M. Borland, APS LS-287 (2000).
- [12] S. Reiche, Nucl. Instr. & Meth. **A429**, 243 (1999).
- [13] Y. Ding, et al., Proc. of IPAC'15, TUPMA003 (2015) and references within.
- [14] D. Ratner et al., PRSTAB **18**, 030704 (2015).